Spectroscopic Determination of the Binding Affinity of Zinc to the DNA-Binding Domains of Nuclear Hormone Receptors†

John C. Payne,‡ Brian W. Rous,‡ Adam L. Tenderholt,‡ and Hilary Arnold Godwin*,‡,§

Department of Chemistry, Northwestern University, 2145 Sheridan Road, Evanston, Illinois 60208-3113, and Department of Biochemistry, Molecular Biology, and Cell Biology, 2153 North Campus Drive, Northwestern University, Evanston, Illinois 60208-3300

Received June 12, 2003; Revised Manuscript Received September 15, 2003

ABSTRACT: Zinc binding to the two Cys_4 sites present in the DNA-binding domain (DBD) of nuclear hormone receptor proteins is required for proper folding of the domain and for protein activity. By utilizing Co^{2+} as a spectroscopic probe, we have characterized the metal-binding properties of the two Cys_4 structural zinc-binding sites found in the DBD of human estrogen receptor α (hERα-DBD) and rat glucocorticoid receptor (GR-DBD). The binding affinity of Co^{2+} to the two proteins was determined relative to the binding affinity of Co^{2+} to the zinc finger consensus peptide, CP-1. Using the known dissociation constant of Co^{2+} from CP-1, the dissociation constants of cobalt from hERα-DBD were calculated: $K_{d1}^{Co} = 2.2 (\pm 1.0) \times 10^{-7}$ M and $K_{d2}^{Co} = 6.1 (\pm 1.5) \times 10^{-7}$ M. Similarly, the dissociation constants of Co^{2+} from GR-DBD were calculated: $K_{d1}^{Co} = 4.1 (\pm 0.6) \times 10^{-7}$ M and $K_{d2}^{Co} = 1.7 (\pm 0.3) \times 10^{-7}$ M. Metal-binding studies conducted in which Zn^{2+} displaces Co^{2+} from the metal-binding sites of hERα-DBD and GR-DBD indicate that Zn^{2+} binds to each of the Cys_4 metal-binding sites approximately 3 orders of magnitude more tightly than Co^{2+} does: the stoichiometric dissociation constants are $K_{d1}^{Zn} = 1 (\pm 1) \times 10^{-10}$ M and $K_{d2}^{Zn} = 5 (\pm 1) \times 10^{-10}$ M for hERα-DBD and $K_{d1}^{Zn} = 2 (\pm 1) \times 10^{-10}$ M and $K_{d2}^{Zn} = 3 (\pm 1) \times 10^{-10}$ M for GR-DBD. These affinities are comparable to those observed for most other naturally occurring structural zinc-binding sites. In contrast to the recent prediction by Low et. al. that zinc binding in these systems should be cooperative [Low, L. Y., Hernández, H., Robinson, C. V., O'Brien, R., Grossmann, J. G., Ladbury, J. E., and Luisi, B. (2002) *J. Mol. Biol. 319*, 87−106], these data suggest that the zincs that bind to the two sites in the DBDs of hERα-DBD and GR-DBD do not interact.

The nuclear hormone receptors constitute an important class of transcription factors that are involved in cellular development, differentiation, and stimulus response in higher eukaryotes (*1*). As a result, the evolution of the nuclear hormone receptors is believed to have been a pivotal event in the development of intercellular communication and the emergence of multicellular organisms (*2*, *3*). Members of the nuclear hormone receptor superfamily play an essential role in the mediation of hormonal signals by acting as intracellular receptors and activating transcription of a variety of genes (*1*, *4*, *5*). In a simplified model, a hormonal ligand binds to a specific nuclear hormone receptor (*5*). The protein−ligand complex then binds, usually as a dimer, to specific DNA sequences, known as hormone response elements, within the promoter regions of genes whose expression is controlled by hormonal activity (*5*).

Nuclear hormone receptors contain five domains: the amino-terminal domain, which features a transcriptional activation region; the DNA-binding domain (DBD);[1] the variable hinge domain; the ligand-binding domain, which features the hormone-binding site, a dimerization region, and a second transcriptional activation site; and a variable carboxy-terminal tail (*1*, *5*, *6*). The ability of each nuclear hormone receptor protein to recognize and bind to specific sequences of DNA is conferred by the DBD. The DBD is highly conserved among members of this protein family and features two, four-cysteine structural zinc-binding sites (*1*, *7*, *8*). In each zinc-binding site, two of the coordinating cysteine residues are located in an α-helix that begins at the third conserved cysteine and extends beyond the fourth

† Supported by NIH Grant 1 R01 GM58183-01A1 (H.A.G.).

* To whom correspondence should be addressed. Phone: (847) 467-3543. Fax: (847) 491-5937. Email: h-godwin@northwestern.edu.

‡ Department of Chemistry.

§ Department of Biochemistry, Molecular Biology, and Cell Biology.

[1] Abbreviations: bis-Tris, bis(2-hydroxyethyl)iminotris(hydroxymethyl)-methane; BRCA1, breast and ovarian cancer susceptibility gene; CP-1, zinc finger consensus peptide that has two histidines and two cysteines in the zinc-binding site (also abbreviated as CP-CCHH); Cys, cysteine; Da, dalton; DBD, DNA-binding domain; DTNB, 5,5′-dithiobis(2-nitrobenzoic acid); DTT, dithiothreitol; E64, trans-epoxysuccinyl-L-leucylamido(4-guanidino)butane; ERE, estrogen response element; ESI-MS, electrospray ionization mass spectrometry; EXAFS, extended X-ray absorption fine structure; GR, glucocorticoid receptor; GR-DBD, glucocorticoid DNA-binding domain; GRE, glucocorticoid response element; GST, glutathione-*S*-transferase; hERα, human estrogen receptor α; hERα-DBD, human estrogen receptor α DNA-binding domain; His, histidine; HPLC, high-performance liquid chromatography; ICP, inductively coupled plasma; IPTG, isopropyl-β-D-thiogalactopyranoside; LFSE, ligand field stabilization energy; LMCT, ligand-to-metal charge transfer; MALDI-TOF MS, matrix-assisted laser desorption and ionization time-of-flight mass spectrometry; PBS, phosphate-buffered saline; PBST, phosphate-buffered saline supplemented with 0.05% (v/v) Tween-20; PCR, polymerase chain reaction; PMSF, phenylmethylsulfonyl fluoride; TCB, thrombin cleavage buffer; ZntR, intracellular zinc metalloregulatory protein from *Escherichia coli.*

10.1021/bi035002l CCC: $25.00
Published on Web 11/11/2003

Table 1: Dissociation Constants for Co^{2+} and Zn^{2+} from a Variety of Structural Zinc-Binding Domains; Values in Parentheses Are Calculated[a]

	K_d Co^{2+} (M)	K_d Zn^{2+} (M)	ref
	Cys_2His_2		
TFIIIA (30-amino acid peptide from transcription factor IIIA)	$3.8 (\pm 0.5) \times 10^{-6}$	$2.8 (\pm 0.9) \times 10^{-9}$	*24*
CP-1 (26-amino acid zinc finger consensus peptide)	$6.3 (\pm 2.2) \times 10^{-8}$	$5.7 (\pm 1.3) \times 10^{-12}$	*27*
	$Cys_2HisCys$		
CP-CCHC (26-amino acid zinc finger consensus peptide)	$6.3 (\pm 2.2) \times 10^{-8}$	$3.2 (\pm 1.0) \times 10^{-12}$	*27*
RMLV (18-amino acid peptide from the nucleocapsid protein of Rauscher murine leukemia virus)	1×10^{-6}	6×10^{-10}	*29*
	$Cys_2HisCys$		
HIV-CCHC (18-amino acid peptide representing N-terminal metal-binding domain of HIV nucleocapsid protein)	9.0×10^{-8}	7.0×10^{-11}	*48*, *55*, *56* [b]
NZF-1 (120-amino acid protein featuring two CCHC domains from neural zinc finger factor 1)	$4 (\pm 2) \times 10^{-7}$ for each domain	$1.4 (\pm 0.8) \times 10^{-10}$ for each domain	*34*
	Cys_4		
CP-CCCC (26-amino acid zinc finger consensus peptide)	$3.5 (\pm 1.0) \times 10^{-7}$	$1.1 (\pm 0.3) \times 10^{-12}$	*27*
	Cys_4·$CysHisCys_2$		
BRCA1 (56-amino acids from BRCA1 gene)			*32*
k_1	2.6×10^{-8}	(2.6×10^{-11})[a]	
k_2	4.5×10^{-7}	(4.5×10^{-10})[a]	
k_3	7.9×10^{-6}	(7.9×10^{-9})[a]	
hdm2 (amino acids 425−491 of hdm2 oncoprotein)			*33*
k_1	2.2×10^{-7}	(2.2×10^{-10})[a]	
k_2	4×10^{-6}	(4×10^{-9})[a]	
k_3	1.0×10^{-7}	(1.0×10^{-10})[a]	

[a] Calculated using reported K_d^{Co} assuming that $K_d^{Zn}/K_d^{Co} = 1 \times 10^{-3}$ (*48*). [b] The values reported here are lower than previously reported values due to the formation of a ternary complex, which is a result of the small, unstructured nature of the HIV-CCHC peptide (*48*).

conserved cysteine (*1*). Both the ER and the GR bind to specific palindromic sites within the DNA as dimers (*1*), and the binding occurs through the helix from the amino terminal structural zinc-binding site (*7*−*10*). Zinc binding to the four-cysteine motifs of the nuclear hormone receptors and to the structural zinc-binding sites found in other proteins is required to stabilize the active conformation of the domain and enables the protein to interact with DNA (*11*−*13*). Members of the nuclear steroid receptor superfamily also contain a ninth conserved cysteine residue in the DBD. However, previous work has suggested that this residue does not participate in metal binding and most likely serves to stabilize the structure of the DBD (*14*).

Despite the fact that the DNA-binding activity of the nuclear hormone receptor proteins is dependent on zinc (*1*, *11*, *15*), little quantitative information is available about the metal-binding properties of these proteins. We are particularly interested in hERα and GR due to the critical roles these proteins play in cellular development and function. For example, the hERα is important to normal reproductive development (*16*, *17*), and the GR is needed for central nervous system, cardiovascular, and metabolic homeostasis (*16*−*18*). Furthermore, the hERα protein has been linked to the onset and progression of breast and ovarian cancers (*19*).

Because of the fact that Zn^{2+} has a d^{10} electron configuration, Zn^{2+} is considered to be spectroscopically silent. However, Co^{2+} (d^7) has proven to be an excellent spectroscopic probe for zinc-binding sites in metalloproteins (*20*). Co^{2+} is an excellent probe for zinc-binding sites because the coordination geometries adopted by Co^{2+} are similar to those adopted by Zn^{2+}. Moreover, the absorption spectrum exhibited by Co^{2+} is very sensitive to its coordination environment, and Co^{2+} substitution for Zn^{2+} often does not disrupt the protein structure or function (*21*−*23*). Thus, the chromophoric properties of Co^{2+} can be used to determine the binding affinity of Zn^{2+} to metal-binding sites found in metalloproteins. The binding affinity of Zn^{2+} for a metal-binding site can be determined by monitoring the declining intensity of the Co^{2+} d → d electronic transitions as Co^{2+} is displaced from the metal-binding site by Zn^{2+} (*24*). The binding affinities of Co^{2+} to structural zinc-binding sites are typically 3−4 orders of magnitude lower than for Zn^{2+} (Table 1).

Co^{2+} has been utilized in the characterization of structural zinc-binding domains in a variety of proteins including zinc finger proteins (*24*−*28*), retroviral nucleocapsid proteins (*29*−*31*), RING finger proteins (*32*, *33*), and a member of the NZF/MyT1 family of neural-specific transcription factors (*34*, *35*) (Table 1). Metal-binding studies conducted with the RING finger domain from the breast and ovarian cancer susceptibility gene (BRCA1) product (*32*) and the RING finger domain of the oncoprotein hdm2 (human form of mdm2, murine double minute chromosome clone number 2) (*33*) demonstrated that metal binding occurs in a thermodynamically sequential fashion in which one metal-binding site within each protein molecule is almost completely saturated before a metal ion binds at the other site. Here, we report the stoichiometric dissociation constants (K_ds, Figure 1) for both Co^{2+} and Zn^{2+} to the two Cys_4 metal-binding sites in hERα-DBD and GR-DBD.

MATERIALS AND METHODS

Preparation of the pGEX·PKT/hERα-DBD Expression Vector. The cDNA for hERα was obtained in the form of the pSG5/HEG0 (*36*) eukaryotic expression vector from Dr. Barry Gehm (Northwestern University Medical School) and Prof. Pierre Chambon (Institut de Genetique et de Biologie Moleculaire et Cellulaire). The cDNA encoding the hERα-DBD (residues 121−280 of the hERα gene) (*37*) was isolated from the pSG5/HEG0 plasmid with the oligonucleotide primers EST-121aa (*38*) and EST-280aa (*39*) by performing PCR on a PTC-100 thermal cycler developed by MJ

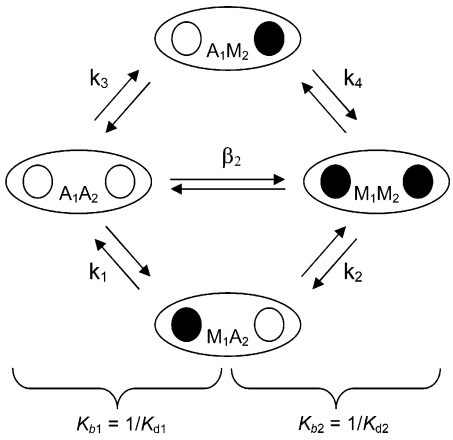

FIGURE 1: General thermodynamic scheme for metal binding to a two-site protein. This scheme depicts the thermodynamic possibilities for two metal ions binding to a protein with two metal binding sites with individual site affinities (k_is), stoichiometric binding constants (K_{b1} and K_{b2}), and stoichiometric stability constants (β_1 and β_2) identified. A refers to apo (metal free) sites, and M refers to metal bound to the site. The subscripts for the individual site affinities (k_is) and site occupancy markers (A_1, A_2, M_1, M_2) refer to the site number; the subscripts in the stoichiometric binding constants (K_1 and K_2) and stoichiometric stability constants (β_1 and β_2) refer to the metal stoichiometry. The following definitions were used (*52*): β = overall stability constant = $[ML_x^{n+}]/[M^{n+}][L]^x$; $\beta_1 = [ML^{n+}]/[M^{n+}][L]$; $\beta_2 = [ML_2^{n+}]/[M^{n+}][L]^2$; etc. K_b = binding constant = $[ML_x^{n+}]/[ML_{x-1}^{n+}][L]$; $K_{b1} = [ML^{n+}]/[M^{n+}][L]$; $K_{b2} = [ML_2^{n+}]/[ML^{n+}][L]$; etc. K_d = dissociation constant = $1/K_b$ where $\beta_1 = K_{b1}$, $\beta_2 = K_{b1} \times K_{b2}$, etc.

Research, Inc. The gel-purified PCR product was subcloned into the *Bam*HI and *Eco*RI restriction sites of the pGEX·PKT prokaryotic expression vector (*40*). The DNA sequence of the resultant pGEX·PKT/hERα-DBD construct was confirmed by automated sequencing using an ABI PRISM 310 Genetic Analyzer (Perkin-Elmer), and the construct was transformed into *Escherichia coli* BL21-CodonPlus-RP cells (Stratagene).

Preparation of the pGEX·PKT/GR-DBD Expression Vector. The cDNA for GR was obtained in the form of the p2A/GRGZ eukaryotic expression vector (*41*) from Dr. Richard Gaber (Department of Biochemistry, Molecular Biology, and Cell Biology at Northwestern University). The cDNA encoding the GR-DBD (residues 425−515 of the GR gene) (*42*) was isolated from the p2A/GRGZ plasmid with the oligonucleotide primers GR-425aa (*43*) and GR-515aa (*44*) by performing PCR on a PTC-100 thermal cycler developed by MJ Research, Inc. The gel-purified PCR product was subcloned into the *Bam*HI and *Eco*RI restriction sites of the pGEX·PKT prokaryotic expression vector (*40*). The DNA sequence of the resultant pGEX·PKT/GR-DBD construct was confirmed by automated sequencing using an ABI PRISM 310 Genetic Analyzer (Perkin-Elmer), and the construct was transformed into *E. coli* BL21-CodonPlus-RIL cells (Stratagene).

Expression and Purification of hERα-DBD Protein. Expression of the GST-hERα-DBD fusion protein in *E. coli* BL21-CodonPlus-RP was induced by adding isopropyl-β-D-thiogalactopyranoside (IPTG) to the cell culture (OD_{600} = 0.5) to a final concentration of 0.1 mM. The cell culture was shaken vigorously at 37 °C for 3 h. The isolated cell pellets were resuspended in phosphate-buffered saline (PBST: 137 mM NaCl, 2.7 mM KCl, 4.3 mM $Na_2HPO_4 \cdot 7H_2O$, 1.4 mM KH_2PO_4 + 0.05% (v/v) Tween-20) supplemented with 0.1% (v/v) 2-mercaptoethanol, 5 mM dithiothreitol (DTT), 5 mM $MgCl_2$, 0.3 mM phenylmethylsulfonyl fluoride (PMSF), 0.5 μg/mL leupeptin, 0.7 μg/mL pepstatin, 2 μg/mL trans-epoxysuccinyl-L-leucylamido(4-guanidino)-butane (E-64), and 1.0 μg/mL aprotinin. The cells were lysed by passing them through an Emulsiflex-C5 High-Pressure Homogenizer (Avestin, Inc.). Sodium deoxycholate and deoxyribonuclease I were added to the cell lysate to concentrations of 0.05% (w/v) and 5 μg/mL, respectively. The cell lysate was incubated at 4 °C for 30 min and then centrifuged at 39 200*g* at 4 °C for 45 min. Polyethylenimine was added to the cell lysate to final concentration of approximately 0.2% (w/v). The solution was clarified at 39 200*g* at 4 °C for 30 min. The supernatant was filtered through a 0.22 μm disposable syringe filter and incubated overnight on a glutathione sepharose column (Amersham Pharmacia Biotech, Inc.) at 4 °C.

The GST affinity tag was cleaved from the GST-hERα fusion protein by incubating the glutathione sepharose column overnight at 4 °C with 50 U of thrombin protease (ICN Biomedicals, Inc.) in 10 mL of thrombin cleavage buffer (TCB: 50 mM Tris·HCl, pH 8; 150 mM NaCl; 2.5 mM $CaCl_2$; 0.1% 2-mercaptoethanol). The protein was eluted from the glutathione sepharose column and purified by gel-filtration chromatography on a Superdex-75 column (Amersham Pharmacia Biotech, Inc.) using a 50 mM Tris·HCl, 100 mM NaCl, 5 mM DTT, pH 7.2 buffer.

The FPLC fractions containing the hERα-DBD were concentrated and dialyzed against a buffer consisting of 6 M urea, 10 mM 1,10-phenanthroline, 1 M acetic acid, and 5 mM DTT, pH 3.0 at 4 °C for 4 h. The apo-protein solution was then dialyzed against purified, metal-free water in an acid-washed, metal-free beaker at 4 °C for 3 h. The water used in this final dialysis was purified with a MilliQ purification system, passed through a column containing Chelex media (Sigma) to remove any trace metals, and then purged with argon. The apo-protein solution was concentrated under vacuum in an inert atmosphere (95% N_2, 5% H_2) chamber.

Less than 0.1 molar equiv of Zn^{2+} was present in the purified hERα-DBD protein sample based on the inductively coupled plasma spectrometric analysis that was performed on a Thermo Jarrell Ash Atomscan Model 25 Sequential ICP Spectrometer. The molecular weight of the hERα-DBD protein (observed 18 421 daltons (Da); calculated 18 420 Da) was confirmed by ESI-MS. The ability of the hERα-DBD to fold and function properly upon the introduction of metal was demonstrated by performing circular dichroism (Supporting Information Figure 5A) and electrophoretic mobility shift assays (Supporting Information Figure 6A).

Expression and Purification of GR-DBD Protein. Expression of the GST-GR-DBD protein in *E. coli* BL21-CodonPlus-RIL cells (Stratagene) was induced by adding isopropyl-β-D-thiogalactopyranoside (IPTG) to the cell culture (OD_{600} = 0.5) to a final concentration of 0.1 mM. The cell culture was shaken vigorously at 37 °C for 3 h. The isolated cell pellets were resuspended in phosphate-buffered saline (PBS: 137 mM NaCl, 2.7 mM KCl, 4.3 mM $Na_2HPO_4 \cdot 7H_2O$, 1.4 mM KH_2PO_4) supplemented with 0.1% (v/v) 2-mercaptoethanol, 5 mM DTT, 5 mM $MgCl_2$, 0.3 mM PMSF, and 1.0 μg/mL aprotinin. The cells were lysed by passing them through an Emulsiflex-C5 High-Pressure

Homogenizer (Avestin, Inc.). Deoxyribonuclease I was added to the cell lysate to a concentration of 5 μg/mL. The cell lysate was incubated at 4 °C for 30 min and then centrifuged at 39 200*g* at 4 °C for 45 min. Polyethylenimine was added to the cell lysate to final concentration of approximately 0.2% (w/v). The solution was then centrifuged at 39 200*g* at 4 °C for 30 min. The supernatant was filtered through a 0.22 μm disposable syringe filter and incubated overnight on a glutathione sepharose column (Amersham Pharmacia Biotech, Inc.) at 4 °C.

The GR-DBD protein was cleaved from its GST affinity tag by incubating the glutathione sepharose column overnight at 4 °C with 50 U of thrombin protease (ICN Biomedicals, Inc.) in 10 mL of TCB. The protein was eluted from the glutathione sepharose column and purified by gel-filtration chromatography on a Superdex-75 column (Amersham Pharmacia Biotech, Inc.) using a 50 mM Tris·HCl, 100 mM NaCl, 5 mM DTT, pH 7.2 buffer.

The FPLC fractions containing the GR-DBD protein were concentrated and dialyzed against a buffer consisting of 6 M urea, 10 mM 1,10-phenanthroline, 1 M acetic acid, and 5 mM DTT, pH 3.0 at 4 °C for 4 h. The apo-protein solution was then dialyzed against purified, metal-free water in an acid-washed, metal-free beaker at 4 °C for 3 h. The water used in this final dialysis was purified with a MilliQ purification system, passed through a column containing Chelex media (Sigma) to remove any trace metals, and then purged with argon. The apo-protein solution was concentrated under vacuum in an inert atmosphere (95% N_2, 5% H_2) chamber.

Less than 0.1 molar equiv of Zn^{2+} was present in the purified GR-DBD protein sample based on the inductively coupled plasma spectrometric analysis that was performed on a Thermo Jarrell Ash Atomscan Model 25 Sequential ICP Spectrometer. The molecular weight of the GR-DBD protein (9962 Da; calculated 9954 Da) was confirmed by MALDI-TOF MS. The ability of the GR-DBD to fold and function properly upon the introduction of metal was demonstrated by performing circular dichroism (Supporting Information Figure 5B) and electrophoretic mobility shift assays (Supporting Information Figure 6B).

Purification of CP-1 by HPLC. The CP-1 zinc finger consensus peptide (*26*, *45*) was purchased from Biosynthesis, Inc. (Lewisville, TX). The peptide was greater than 70% pure as purchased, and the molecular weight of the peptide had been confirmed by mass spectrometry (2972.0 Da; calculated 2962.4 Da). Prior to conducting the metal-binding studies, the peptide was reduced and further purified by reverse phase HPLC. Five milligrams of the peptide was dissolved in 500 μL of metal-free water, which was purified with a MilliQ purification system and passed through a column containing Chelex media (Sigma) to remove any trace metals. Ten molar equiv of DTT was added to the peptide solution, and the peptide solution was incubated at 55 °C for 2 h. The peptide solution was filtered through a 0.22 μm disposable syringe filter and injected onto a Rainin Dynamax C18 column. The homogeneous peptide fraction was collected from the C18 column and taken into an inert atmosphere chamber where it was concentrated under vacuum.

Reagents Used in Metal-Binding Titrations of hERα-DBD and GR-DBD. The solutions used in the metal-binding experiments were prepared with metal-free reagents and water that was purified with a MilliQ purification system and passed through a column containing Chelex media (Sigma) to remove trace metals. A $CoCl_2$ stock solution was prepared by dissolving $CoCl_2$ (Aldrich, 99.999%) in purified, metal-free water, and the concentration of the solution was determined by measuring the absorption intensity of the solution at 512 nm ($\epsilon_{512} = 4.8\ M^{-1}\ cm^{-1}$) (*21*). A Zn^{2+} atomic absorption standard (Aldrich, 15.25 mM Zn^{2+} in 1.0% HCl) was utilized in the metal competition experiments. Each metal-binding titration was performed in 100 mM bis-Tris, pH 7.4. All solutions were purged with helium prior to being introduced into the inert atmosphere chamber where they were stored and handled at all times.

Concentration Determination of hERα-DBD. The concentration of hERα-DBD present in each sample was determined by measuring the absorption intensity of the protein sample at 280 nm ($\epsilon_{280} = 20\,900\ M^{-1}\ cm^{-1}$) using a Cary 300 Bio UV−vis spectrophotometer or a Cary 500 UV−vis−NIR spectrophotometer. The extinction coefficient of hERα-DBD (at 280 nm = $20\,900\ M^{-1}\ cm^{-1}$) was determined by amino acid analysis conducted by the Keck Biophysics Facility at Yale University.

Concentration Determination of GR-DBD. The approximate concentration of reduced GR-DBD was determined by performing a 5,5′-dithiobis(2-nitrobenzoic acid) (DTNB) colorimetric assay (*46*). A GR-DBD protein solution was prepared by dissolving the pure protein in 150 μL of metal-free water. A total of 2 μL of this solution was added to a cuvette containing 1000 μL of 100 mM, pH 7.4, bis-Tris buffer and 100 μL of a 5 mM DTNB solution. The DTNB was allowed to react with the GR-DBD for 30 min in an anaerobic environment. Each free thiol group present in the GR-DBD protein yields 1 equiv of TNB^{2-} ($\epsilon_{412}(TNB^{2-}) = 14\,150\ M^{-1}\ cm^{-1}$). This method did not provide reliable results when used with the hERα-DBD.

Concentration Determination of CP-1. The concentration of the reduced CP-1 zinc finger consensus peptide was determined by saturating a portion of the peptide sample with Co^{2+}. The absorption intensity of the Co·CP-1 solution was measured at 640 nm on a Hewlett-Packard 8453 diode array spectrophotometer, and the concentration of the reduced peptide stock solution was calculated utilizing the molar extinction coefficient of the Co·CP-1 complex ($\epsilon_{640} = 900\ M^{-1}\ cm^{-1}$) (*47*).

Metal-Binding Titrations of hERα-DBD and GR-DBD. Absorption spectra collected during the course of the metal-binding experiments were recorded from 250 to 900 nm on a Cary 300 Bio UV−vis spectrophotometer or a Cary 500 UV−vis−NIR spectrophotometer at 37 °C. To characterize the metal-binding properties of hERα-DBD and GR-DBD, aliquots containing 0.2 molar equiv of Co^{2+} (relative to the amount of protein present, approximately 40 μM) were added to the protein solution, and an absorption spectrum was collected after each addition. This process was repeated until the ligand-field absorption bands no longer increased in intensity, indicating that the protein was saturated with Co^{2+} (approximately 2.4 molar equiv of Co^{2+}). Two more aliquots of the Co^{2+} solution, each containing 0.4 molar equiv of Co^{2+}, were added to the protein solution to ensure that the sample was completely saturated.

For the studies in which the binding constants of Co^{2+} to the two Cys_4 metal-binding sites of hERα-DBD and GR-

DBD were determined, the CP-1 zinc finger consensus peptide was mixed with the protein in an approximately 2:1 ratio so that the peptide could serve as a competing ligand for each of the Cys_4 sites. Aliquots containing 0.25 molar equiv of Co^{2+} (relative to the amount of protein present) were sequentially added to protein/CP-1 mixture. The metal−peptide−protein solution was incubated at 37 °C following the addition of each aliquot of Co^{2+} until there were no noticeable changes in the absorption spectrum (approximately 10−15 min), indicating that equilibrium had been reached. The intensity of the ligand-field absorption bands stopped increasing after approximately 4.00−4.25 molar equiv of Co^{2+} had been added, but a total of 6.00 molar equiv of Co^{2+} was added to ensure that the peptide/protein mixture was saturated with metal.

The ability of Zn^{2+} to compete with Co^{2+} for the Cys_4 metal-binding sites of hERα-DBD and GR-DBD was assessed by titrating aliquots of the Zn^{2+} atomic absorption solution into a cuvette containing the Co^{2+}-protein complex along with a 200-fold molar excess of Co^{2+} relative to the amount of protein present. Excess Co^{2+} was added to the solution to increase the competition between Zn^{2+} and Co^{2+} for the two metal-binding sites in each protein (*48*). The excess Co^{2+} was accounted for quantitatively using the fitting program SPECFIT/32. An absorption spectrum was collected after the addition of each aliquot of the Zn^{2+} standard solution to monitor the displacement of Co^{2+} by Zn^{2+} from the metal-binding sites. The metal-protein solution was incubated at 37 °C until there were no noticeable changes in the absorption spectrum (approximately 10−15 min), indicating that equilibrium had been reached. Zn^{2+} was titrated into the protein solution until the intensity of the ligand-field absorption bands had decreased to baseline levels (approximately 11.0 molar equiv of Zn^{2+}).

Analysis of Metal-Binding Studies. The resulting absorption spectra were analyzed using the fitting program SPECFIT/32 (*49*). SPECFIT/32 determines the number of colored species that contribute to the absorption spectra using a factor analysis procedure. SPECFIT/32 fits all wavelengths simultaneously to obtain a best fit, although the comparison of the fit to the data is only shown for one wavelength (739 nm). For the titrations reported herein, fits were obtained from the region of the spectrum corresponding to the Co^{2+} d → d transitions (550−800 nm). These features are excellent markers for the Co-protein because no apo-protein absorptions are observed in this region. For each titration, the fitting results at different wavelengths were also checked to make certain that the fit qualitatively matched the experimental data. SPECFIT/32 calculates model-dependent binding constants for each species present in solution. The model created to fit the Co^{2+} titrations of the hERα-DBD/CP-1 solution accounts for the formation of the Co·CP-1, Co·hERα-DBD, Co_2·hERα-DBD, and Co·bis-Tris complexes. Similarly, the model created to fit the Co^{2+} titrations of the GR-DBD/CP-1 mixture accounts for the formation of the Co·CP-1, Co·GR-DBD, Co_2·GR-DBD, and Co·bis-Tris complexes. In each analysis, the apo-protein absorbance spectrum (absorbance band at 280 nm) was subtracted from all spectra obtained during the course of the titration. The subtraction was normalized with respect to the decreasing apo-protein concentration. Furthermore, the exact concentrations of reduced hERα-DBD and GR-DBD used in the titrations were adjusted based on the Co^{2+} titration data curves produced by SPECFIT/32.

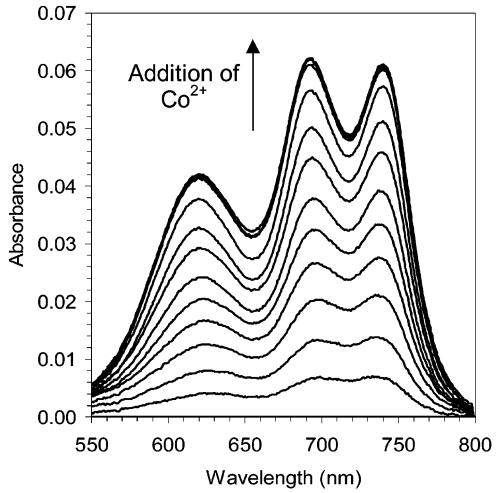

FIGURE 2: Absorption spectra collected during a Co^{2+} titration of hERα-DBD (46.3 μM) in 100 mM bis-Tris, pH 7.4 at 37 °C. The absorption spectrum of the apo-protein was subtracted from each spectrum collected during the course of the metal-binding titration. Similar data for GR-DBD are available in the Supporting Information.

The model created to analyze the Co^{2+}/Zn^{2+} competition studies assumes that the Co_2·hERα-DBD (or Co_2·GR-DBD) and the Co·bis-Tris complexes are initially present, and the Co·Zn·hERα-DBD and Zn_2·hERα-DBD (or Co·Zn·GR-DBD and Zn_2·GR-DBD) complexes are formed during the course of the experiment. The binding affinities of Co^{2+} and Zn^{2+} to the bis-Tris buffer (Co^{2+} log $\beta_1 = 1.8$; Zn^{2+} log $\beta_1 = 2.4$) (*50*) and a known basis spectrum of the Co·bis-Tris complex, which absorbs weakly in the visible region, were included in the binding models.

RESULTS

Titration of the hERα-DBD (Figure 2) and GR-DBD with Co^{2+} (Supporting Information Figure 2) resulted in the absorption spectra shown in Figure 3A,B, respectively. The intensity ($\epsilon \sim 1000$ M^{-1} cm^{-1}, Figure 2) and the position of the Co^{2+} d → d electronic transitions observed between 550 and 800 nm indicate that Co^{2+} is coordinated by the protein in a tetrahedral environment. Co^{2+}-binding studies conducted with other tetrahedral, structural zinc-binding domains have yielded similar absorption spectra (*13*, *21*, *22*, *24*, *32*). It is also apparent from the absorption spectra that Co^{2+} binds to hERα-DBD and GR-DBD in a 2:1 ratio as Zn^{2+} does. The intensity of the Co^{2+} d → d electronic transitions stopped increasing once approximately two molar equiv of Co^{2+} had been added to the protein solutions.

As Co^{2+} is titrated into a solution containing hERα-DBD, the shape of the ligand-field absorption bands changes (Figure 2). Initially, the middle ligand-field absorption band (699 nm) has a weaker absorption intensity than the lowest energy absorption band (739 nm). However, as the Co^{2+}/hERα-DBD ratio approaches two, the middle absorption band shifts to a higher energy position (692 nm), and it becomes more intense than the lowest energy absorption band (739 nm). The highest energy ligand-field absorption band also shifts to a higher energy position, from 626 to 618 nm, as the Co^{2+}/hERα-DBD ratio approaches two.

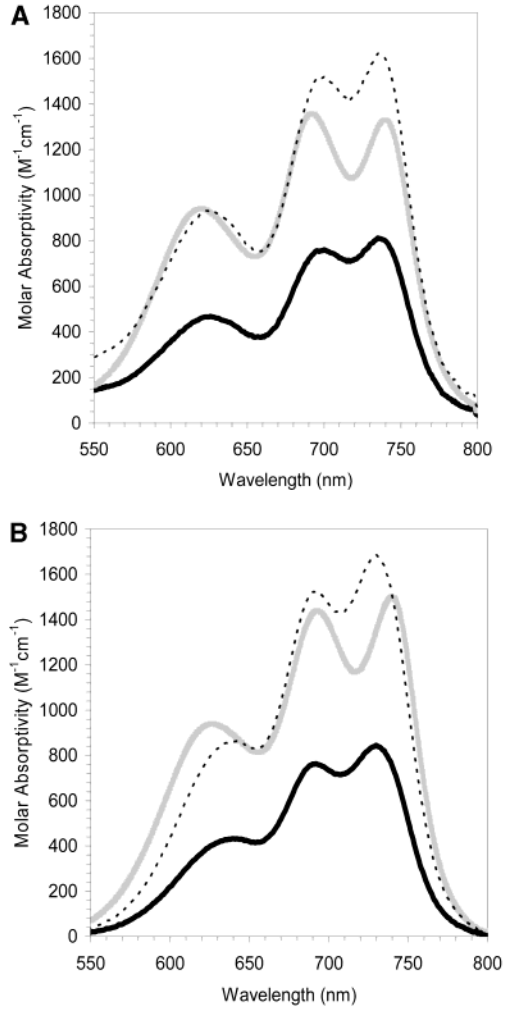

FIGURE 3: Ligand-field absorption bands exhibited by the (A) Co·hERα-DBD (black solid line) and Co_2·hERα-DBD (gray solid line) complexes and (B) Co·GR-DBD (black solid line) and Co_2·GR-DBD (gray solid line) complexes, which were deconvoluted by the fitting program, SPECFIT/32, from the absorption spectra collected during Co^{2+} titrations of the hERα-DBD and GR-DBD proteins. Note that the shapes of the absorption bands change during the course of the titration. The Co_2·hERα-DBD and Co_2·GR-DBD spectra differ significantly from two times the 1:1 Co·hERα-DBD and 1:1 Co·GR-DBD complexes (dotted lines; ···) that are observed experimentally.

Similarly, the positions of the ligand-field absorption bands change as Co^{2+} is titrated into a solution containing GR-DBD (Supporting Information Figure 2). At the beginning of the titration, the lowest energy and highest energy absorption bands are located at 739 and 640 nm, respectively However, as the Co^{2+}/GR-DBD ratio approaches two, the highest energy absorption band shifts to a higher energy position (630 nm), and the lowest energy absorption band shifts to a lower energy position (749 nm). Such differences in the Co^{2+} absorbance spectra between GR-DBD and hERα-DBD are not unexpected because Co^{2+} d → d electronic transitions are extremely sensitive to the exact environment of the Co^{2+}.

Two basis spectra, which were assigned to the Co·hERα-DBD and Co_2·hERα-DBD complexes, were imported into SPECFIT/32 from the absorption spectra collected during the Co^{2+} titrations of hERα-DBD (Figure 3A). Similarly, two basis spectra were imported into SPECFIT/32 from the Co^{2+} titrations of GR-DBD and were assigned to the Co·GR-DBD and Co_2·GR-DBD complexes (Figure 3B). When the experimental spectrum obtained halfway through the titration (i.e., when Co/ER-DBD or Co/GR-DBD is 1:1) is compared to the final experimental spectrum (i.e., when Co/ER-DBD or Co/GR-DBD is 2:1), differences in the shape(s) of the ligand-field absorption bands are readily apparent (Figure 3). This suggests both that a spectral intermediate (Co·hERα-DBD or Co·GR-DBD) is present in these titrations and that the two Cys_4 binding sites in hERα-DBD and GR-DBD bind Co^{2+} with different affinities.

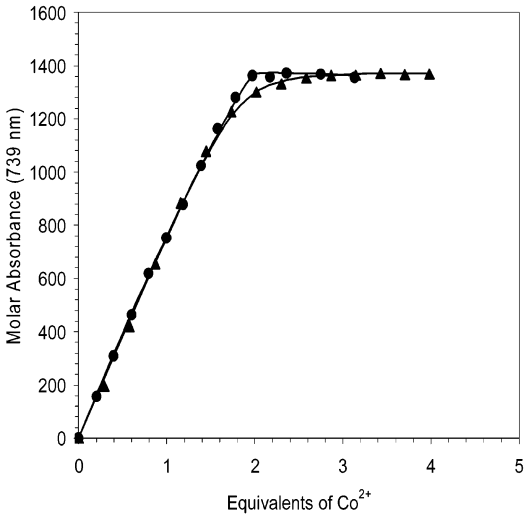

FIGURE 4: Comparison of the calculated fit (line) to the observed absorption intensity at 739 nm from Co^{2+} titrations of hERα-DBD (46.3 μM) (●) and GR-DBD (35.0 μM) (▲).

The spectra obtained during the Co^{2+} titrations of hERα-DBD and GR-DBD were fit using the program SPECFIT/32 (Figure 4). Because of the strong binding interaction between Co^{2+} and two Cys_4 metal-binding sites of hERα-DBD and GR-DBD, only an upper limit for the dissociation constant ($\sim 10^{-7}$ M) can be obtained from the direct Co^{2+} titrations of the proteins. However, by conducting a competition experiment in which Co^{2+} is titrated into a solution containing the apo-protein and a second ligand whose binding affinity for Co^{2+} is known, the dissociation constants for Co^{2+} to the Cys_4 metal-binding sites of hERα-DBD and GR-DBD can be calculated relative to the known value of the competitor ligand (*27*, *51*).

The zinc finger consensus peptide, CP-1, which features one Cys_2His_2 metal-binding site, was used as the competing ligand at a 2:1 molar ratio relative to the amount of protein present so that the zinc finger consensus peptide could compete with each of the Cys_4 metal-binding sites of hERα-DBD or GR-DBD. CP-1 was chosen as the competing ligand because the peptide's binding affinity for Co^{2+} has previously been determined ($K_d = 6.3 \times 10^{-8}$ M) (*27*). In addition, the absorption spectrum exhibited by the Co·CP-1 complex (*27*) is quite distinct from the absorption spectra exhibited by the Co·hERα-DBD and Co_2·hERα-DBD complexes (Figure 5A) and the Co·GR-DBD and Co_2·GR-DBD complexes (Supporting Information Figure 3). Spectra of the Co·CP-1, Co·hERα DBD, and Co_2·hERα-DBD complexes (Figure 5A) were imported into SPECFIT/32 and used as basis spectra to deconvolute the collected absorption spectra for the competition experiment with CP-1 and used to determine the relative binding constants of Co^{2+} to hERα-DBD. The

Table 2: Relative Stability Constants for Co^{2+} and Zn^{2+} Binding to hERα-DBD and GR-DBD[a,b]

	β_1 Co_1(P)/ β_1 Co(CP1)	β_2 Co_2(P)/ β_1 Co(CP1)	β_1 Zn_1(P)/ β_1 Co_1(P)	β_2 Zn_2(P)/ β_2 Co_2(P)
hERα-DBD	0.32	5.0×10^5	1.3×10^3	1.7×10^6
GR-DBD	0.15	1.0×10^6	6.3×10^2	1.5×10^6

[a] β_1 = [MP]/[M][P], where M + P ⇆ MP. [b] β_2 = [M_2P]/[M]^2[P], where 2M + P ⇆ M_2P.

shape of the ligand-field absorption bands that emerged after a few aliquots of the Co^{2+} solution were added to the peptide/protein solution indicate that Co^{2+} binds more tightly to CP-1 than to hERα-DBD (Figure 5B). Consistent with this observation, a quantitative analysis of these competition studies yielded the ratio of the dissociation constants of Co^{2+} from hERα-DBD (K_{d1}^{Co}, K_{d2}^{Co}) to the Co·CP-1 dissociation constant (K_d^{CP-1}): $K_{d1}^{Co}/K_d^{CP-1} = 3.5$ (± 1.6); $K_{d2}^{Co}/K_d^{CP-1} = 10$ (± 2) (Table 2). These values were calculated from the relative stability constants in Table 2 from the following relationships: $K_{d1} = [M][P]/[MP] = 1/K_{b1} = 1/\beta_1$ and $K_{d2} = [M][MP]/[M_2P] = (1/\beta_2)([MP]/[M][P]) = \beta_1/\beta_2 = K_{b1}/\beta_2$, where

$$\beta_1 Zn(P) = \beta_1 Co(CP) \times \left(\frac{\beta_1 Zn_1(P)}{\beta_1 Co_1(P)}\right),$$

$$\beta_2 Co(P) = \beta_1 Co(CP) \times \left(\frac{\beta_2 Co_2(P)}{\beta_1 Co_1(P)}\right),$$

$$\beta_2 Zn_2(P) = \beta_2 Co_2(P) \times \left(\frac{\beta_2 Zn_2(P)}{\beta_2 Co_2(P)}\right)$$

and $\beta_1 Co(CP) = 1.58 \times 10^7$ M (*27*). The absolute values of the dissociation constants of Co^{2+} from hERα-DBD were then calculated using the known dissociation constant for Co·CP-1 ($K_d^{CP-1} = 6.3 \times 10^{-8}$ M) (*27*) and the ratios determined from the competition experiments: $K_{d1}^{Co} = 2.2$ (± 1.0) $\times 10^{-7}$ M and $K_{d2}^{Co} = 6.1$ (± 1.5) $\times 10^{-7}$ M (Table 3). Note that these constants are stoichiometric constants, not site specific constants (Figure 1), because studies were performed on intact protein and not on the isolated sites (*52*). A comparison of the fit calculated by SPECFIT/32 to the experimental data for the competition experiment with CP-1 is provided in Figure 5C. Similarly, analysis of the competition studies between GR-DBD and CP-1 (Supporting Information Figure 3) yielded the ratio of the dissociation constants of Co^{2+} from GR-DBD (K_{d1}^{Co}, K_{d2}^{Co}) to the Co·CP-1 dissociation constant (K_d^{CP-1}): $K_{d1}^{Co}/K_d^{CP-1} = 6.5$ (± 0.9) and $K_{d2}^{Co}/K_d^{CP-1} = 3$ (± 1) (Table 2). The absolute values of the dissociation constants of Co^{2+} from GR-DBD were then calculated using the known dissociation constant for Co·CP-1 ($K_d^{CP-1} = 6.3 \times 10^{-8}$ M) (*27*) and the ratios determined from the competition experiments: $K_{d1}^{Co} = 4.1$ (± 0.6) $\times 10^{-7}$ M and $K_{d2}^{Co} = 1.7$ (± 0.3) $\times 10^{-7}$ M (Table 3). A comparison of the fit calculated by SPECFIT/32 to the original data obtained for this competition study is provided in Figure 5C. The higher molar absorbance observed at saturation in the titration of GR-DBD versus ER-DBD is a result of a larger concentration of CP-1 in the GR-DBD competition experiments. To determine the binding affinity of Zn^{2+} relative to Co^{2+} for the Cys_4 metal-binding sites of hERα-DBD and GR-DBD, Zn^{2+} was titrated in 0.2−

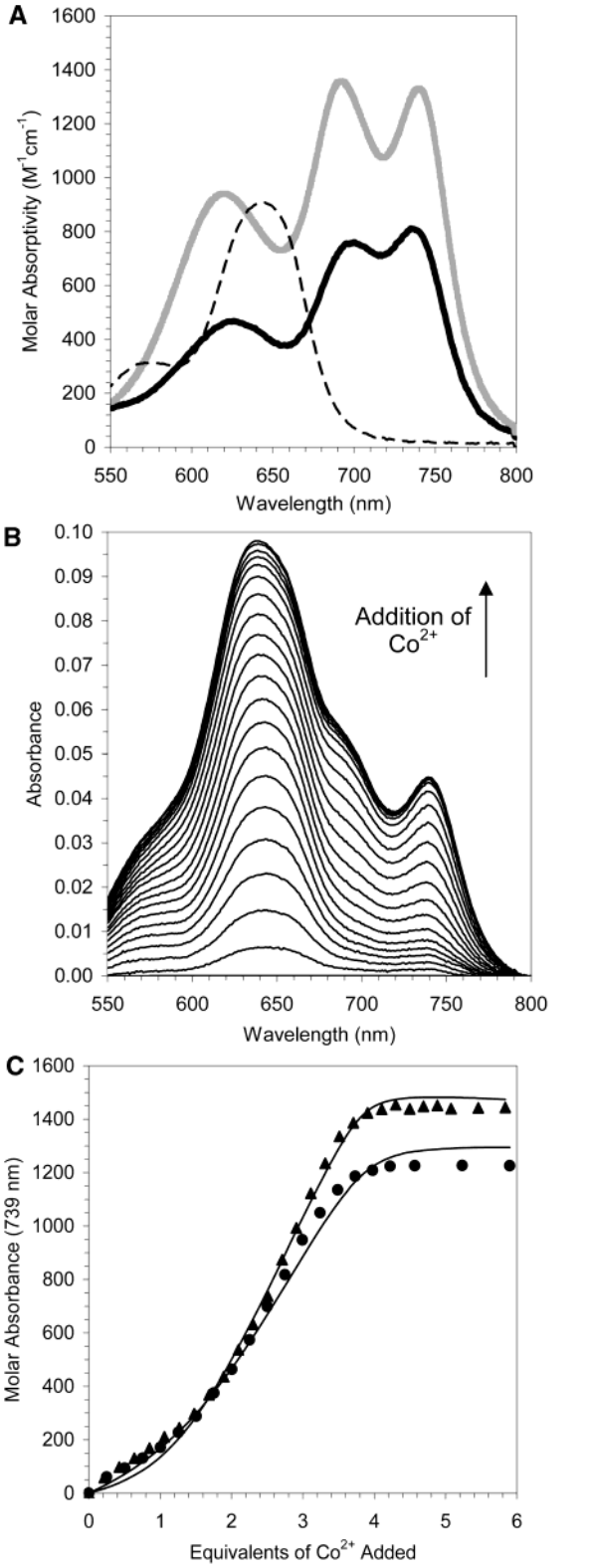

FIGURE 5: (A) Ligand-field absorption bands exhibited by the Co·hERα-DBD complex (black solid line), Co_2·hERα-DBD complex (gray solid line), and the Co·CP-1 complex (dashed line; − − −). (B) Absorption spectra collected during a Co^{2+} titration of a peptide/protein solution containing hERα-DBD (37.9 μM) and a zinc finger consensus peptide, CP-1 (75.8 μM), in 100 mM bis-Tris, pH 7.1 at 37 °C. The absorption spectrum of the apo-protein was subtracted from each spectrum collected during the course of the metal-binding titration. (C) Comparison of the observed data (circles/triangles) to the best fit (lines) obtained from SPECFIT/32 for the Co^{2+} titration of the hERα-DBD /CP-1 mixture (●) and for the Co^{2+} titration of the GR-DBD/CP-1 mixture (▲).

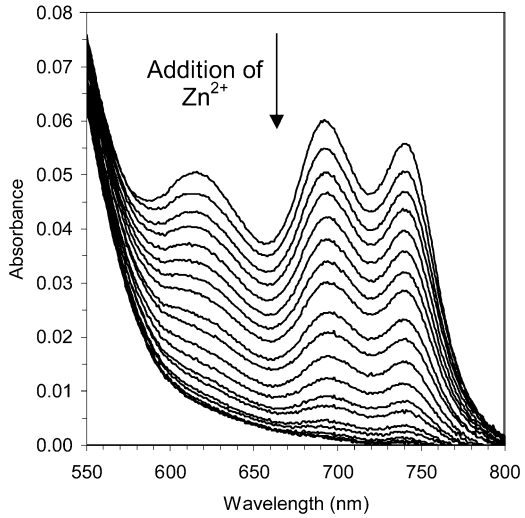

FIGURE 6: Absorption spectra collected during a Zn^{2+} titration of hERα-DBD (45.6 μM) in the presence of approximately 200 molar equiv of Co^{2+} relative to the amount of protein present. The titration was conducted in 100 mM bis-Tris, pH 7.1 at 37 °C. The absorption spectrum of the apo-protein was subtracted from each spectrum collected during the course of the metal-binding titrations.

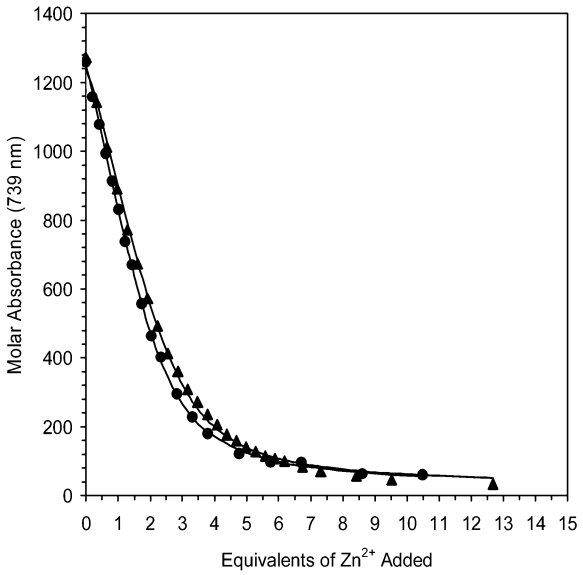

FIGURE 7: Comparison of the observed data to the best fit (line) obtained from SPECFIT/32 for a Co^{2+}/Zn^{2+} competition experiment: (●) hERα-DBD and (▲) GR-DBD.

2.0 equiv aliquots into a solution containing either hERα-DBD (Figure 6) or GR-DBD (Supporting Figure 4) protein saturated with 200 molar equiv of Co^{2+}. Even with such a large excess of Co^{2+} present, the intensity of the absorption bands attributable to the Co·hERα-DBD or Co·GR-DBD complexes gradually declined as Zn^{2+} was added to the protein solution, indicating that the Cys_4 metal-binding sites of hERα-DBD and GR-DBD possess a larger binding affinity for Zn^{2+} than for Co^{2+}.

The binding model constructed for the analysis of the Co^{2+}/Zn^{2+} competition experiments allowed for the presence of the three colored species present in the metal-protein solutions during the course of the experiment: the Co·bis-Tris species; the Co_2·protein complex, which is present at the beginning of the competition study; and a mixed-metal complex, Co·Zn·protein, which is formed as Zn^{2+} initially displaces Co^{2+} from the hERα-DBD and GR-DBD proteins. The Zn_2·protein complex, which does not exhibit ligand-field transitions, was also included in the binding model. The dissociation constants of Zn^{2+} from each Cys_4 site of hERα-DBD and GR-DBD were calculated from the binding model created, and this model provided the best fit to the data (Figure 7). Analysis of the metal competition studies yielded the ratio of the dissociation constants of Zn^{2+} to Co^{2+}. The absolute values of the dissociation constants of Zn^{2+} from hERα-DBD and GR-DBD were calculated from the ratios, and the dissociation constants for the Co-protein complexes were determined from the CP-1 competition binding studies (Table 3). For hERα-DBD, $K_{d1}^{Zn} = 1 (\pm 1) \times 10^{-10}$ M and $K_{d2}^{Zn} = 5 (\pm 1) \times 10^{-10}$ M; for GR-DBD, $K_{d1}^{Zn} = 2 (\pm 1) \times 10^{-10}$ M and $K_{d2}^{Zn} = 3 (\pm 1) \times 10^{-10}$ M.

DISCUSSION

Co^{2+} was utilized as a spectroscopic probe for the Cys_4 metal-binding sites of hERα-DBD and GR-DBD to determine the affinity of both Co^{2+} and Zn^{2+} for these proteins. Circular dichroism experiments (Supporting Information Figure 5) and electrophoretic mobility shift assays (Supporting Information Figure 6) using Co_2·hERα-DBD and Co_2·GR-DBD demonstrate that Co^{2+} is a functional substitution for Zn^{2+} in these proteins. When Co^{2+} is titrated into a solution containing hERα-DBD or GR-DBD, the absorption spectra exhibited by the metal-protein solution (Figure 2) demonstrate that Co^{2+} is a suitable spectroscopic probe for the domain. The position of the three ligand-field absorption bands (618, 692, and 739 nm), which correspond to Co^{2+} electron transitions from the $^4A_2$ to $^4T_1(P)$ state, suggests that each Co^{2+} ion is coordinated by four cysteine residues (*21*, *27*). The ligand-field absorption envelope is red-shifted relative to the transitions observed in studies of complexes formed between Co^{2+} and peptides that feature Cys_2His_2 (573 and 642 nm, e.g., CP-1) (*27*) or $Cys_2HisCys$ (599, 649, and 725 nm) (*27*) metal-binding sites. The observed shift in the energies of the d → d electronic transitions is attributable to the fact that a thiolate ligand is a weaker field ligand than an imidazole (*27*, *53*, *54*). As cysteine residues are substituted for histidine residues at the metal coordination site, Δt, the splitting between the *e* and the t_2 sets of d orbitals in a tetrahedral Co^{2+} complex, decreases, and the energies of the ligand-field transitions decrease (*27*, *53*, *54*).

Furthermore, the visible absorption spectra exhibited by the Co-hERα-DBD and Co-GR-DBD complexes are similar to the visible absorption spectra exhibited by other Co·Cys_4 complexes that have been previously characterized (*22*). The intense absorption band (310 nm) in the near-UV region of the electromagnetic spectrum resembles absorption bands that have been assigned as Cys S^- → Co^{2+} ligand-to-metal charge-transfer (LMCT) bands in other complexes formed between cobalt and zinc-binding sites that feature cysteine residues (*22*, *31*). In conclusion, our experimental observations indicate that Co^{2+} is a suitable spectroscopic probe to qualitatively and quantitatively assess the metal-binding characteristics of hERα-DBD and GR-DBD.

Figure 1 represents the thermodynamic scheme for metal binding to hERα-DBD and GR-DBD. In this scheme, four distinct thermodynamic mechanisms are possible: (1) M^{2+} may bind in a cooperative fashion ($k_2 > k_3$ or $k_4 > k_1$); (2) M^{2+} may bind in an anticooperative fashion ($k_2 < k_3$ or k_4

Table 3: Calculated Stoichiometric Dissociation Constants of hERα-DBD and GR-DBD[a,b]

	K_{d1} Co	K_{d2} Co	K_{d1} Zn	K_{d2} Zn
hERα-DBD	$2.2 (\pm 1.0) \times 10^{-7}$ M	$6.1 (\pm 1.5) \times 10^{-7}$ M	$1 (\pm 1) \times 10^{-10}$ M	$5 (\pm 1) \times 10^{-10}$ M
GR-DBD	$4.1 (\pm 0.6) \times 10^{-7}$ M	$1.7 (\pm 0.3) \times 10^{-7}$ M	$2 (\pm 1) \times 10^{-10}$ M	$3 (\pm 1) \times 10^{-10}$ M

[a] $K_{d1} = [M][P]/[MP] = 1/K_{b1} = 1/\beta_1$. [b] $K_{d2} = [M][MP]/[M_2P] = (1/\beta_2)([MP]/[M][P]) = \beta_1/\beta_2 = K_{b1}/\beta_2$, where $\beta_1Zn(P) = \beta_1Co(CP) \times (\beta_1Zn_1(P)/\beta_1Co_1(P))$; $\beta_2Co(P) = \beta_1Co(CP) \times (\beta_2Co_2(P)/\beta_1Co_1(P))$; $\beta_2Zn_2(P) = \beta_2Co_2(P) \times (\beta_2Zn_2(P)/\beta_2Co_2(P))$; $\beta_1Co(CP) = 1.58 \times 10^7$ M (*27*); relative stability constants are reported in Table 2.

$< k_1$); (3) if M^{2+} binds and the sites do not interact, then it is possible that the two sites are independent and have nonidentical binding affinities ($k_2 = k$, $k_1 = k_4$, and $k_1 \neq k_2$); (4) alternatively, it is possible that the sites do not interact but have identical binding affinities ($k_1 = k_2 = k_3 = k_4$). This scheme highlights the significance of experimentally detecting a distinct Co-protein intermediate species. If a Co-protein spectral intermediate (M_1A_2 or M_2A_1 in Figure 1) is observed during the course of the titration, then $M_1A_2 \neq M_2A_1 \neq M_1M_2/2$ and both β_1 (K_1 in Figure 1) and β_2 (K_2 in Figure 1) can be determined. However, the presence of a spectral intermediate does not necessarily provide a full description of the thermodynamics of metal-binding to the protein (i.e., cooperative vs anticooperative). To fully describe the thermodynamics of metal-binding to a two-site protein, the affinity constants of the isolated sites need to be measured.

If metal binding occurred at the Cys_4 sites of hERα-DBD and GR-DBD in an all or none fashion, then the ligand-field absorption bands attributable to each site would emerge simultaneously, and both sets of absorption bands would gradually increase in intensity as Co^{2+} was titrated into the protein solution. Since one Cys_4 metal-binding site would be occupied at the same rate as the other Cys_4 metal-binding site, the shape of the observed absorption spectra would not change during the course of the titration. The presence of a spectral intermediate during the Co^{2+} titrations of hERα-DBD and GR-DBD indicates that the two Cys_4 metal-binding sites found in the DBDs of these proteins have different metal affinities.

However, calculation of the absolute values of the dissociation constants of Co^{2+} from hERα-DBD and GR-DBD from the competition experiments with CP-1 revealed that the affinity of Co^{2+} for the two sites within a given domain are within a order of magnitude of each other ($K_{d1}^{Co} = 2.2 (\pm 1.0) \times 10^{-7}$ M and $K_{d2}^{Co} = 6.1 (\pm 1.5) \times 10^{-7}$ M for hERα-DBD and $K_{d1}^{Co} = 4.1 (\pm 0.6) \times 10^{-7}$ M and $K_{d2}^{Co} = 1.7 (\pm 0.3) \times 10^{-7}$ M for GR-DBD); the same was true for Zn^{2+} $K_{d1}^{Zn} = 1 (\pm 1) \times 10^{-10}$ M and $K_{d2}^{Zn} = 5 (\pm 1) \times 10^{-10}$ M for hERα-DBD and $K_{d1}^{Zn} = 2 (\pm 1) \times 10^{-10}$ M and $K_{d2}^{Zn} = 3 (\pm 1) \times 10^{-10}$ M for GR-DBD). This behavior contrasts with the marked anticooperativity observed between the two metal binding sites and the RING finger domains from BRCA1 and hdm2 (human homologue of the p53 inhibitor, mdm2 (murine double minute chromosome clone number 2)) (*33*) and suggests that, even though the DNA-binding domain from steroid receptor proteins acts as one functional unit that binds two metal ions (*7*), there is relatively little communication between the two metals as they bind to the two structural zinc-binding sites (i.e., the binding of one metal does not affect the binding of the second metal). This observation contrasts the report by Low et. al. (*14*), which states that both the folding of the ER-DBD and the folding of the GR-DBD occurs via a two-state process, and metal binding occurs in a cooperative manner. The results presented herein suggest that while the folding of the hERα-DBD and GR-DBD domains may occur in a cooperative manner (as suggested by Low et al. (*14*)), the binding of zinc to the two sites in one domain is not cooperative.

The competition experiments between hERα-DBD and CP-1 or GR-DBD and CP-1 allow the affinities of Co^{2+} and Zn^{2+} for these proteins to be directly compared: cobalt binding is slightly weaker for each of the Cys_4 sites within GR-DBD ($K_{d1}^{Co}/K_d^{CP-1} = 6.5 (\pm 0.9)$ and $K_{d2}^{Co}/K_d^{CP-1} = 3 (\pm 1)$) and hERα-DBD ($K_{d1}^{Co}/K_d^{CP-1} = 3.5 (\pm 1.6)$ and $K_{d2}^{Co}/K_d^{CP-1} = 10 (\pm 2)$) than CP-1. Similar results have been reported for a wide range of other naturally occurring structural zinc-binding domains, including proteins with both Cys_2His_2 (TFIIIA and CP-1) (*24*, *27*) and $Cys_2HisCys$ (CP-CCHC, RMLV, HIV-CCHC, and NZF-1) (*27*, *29*, *34*, *55*, *56*) sites (Table 1). Because the ratio of K_d^{Zn} to K_d^{Co} is approximately equal to 1×10^{-3} (*48*), estimates for K_d^{Zn} can be calculated for those proteins for which only K_d^{Co} values have been reported (Table 1, values in parentheses). These results confirm the observation by Krizek and Berg, based on results from a series of consensus peptides in which only the metal-binding residues were varied, that varying the number of cysteines residues in the metal-binding site does not have a significant impact on the affinity of Co^{2+} or Zn^{2+} for structural zinc-binding sites. The K_ds for eukaryotic structural zinc-binding domains are surprisingly consistent regardless of whether the binding site is Cys_2His_2, $Cys_2HisCys$, or Cys_4, with all of the zinc dissociation constants reported for naturally occurring zinc sites falling in the range of 10^{-11} to 10^{-9} M. Taken together, these data, combined with the observation that metal ions exchange rapidly in these sites under physiologically relevant conditions (*48*, *57*), suggest that the concentration of bioavailable zinc in the nucleus of cells cannot be lower than $\sim 10^{-12}$ M.

By contrast, Zn^{2+} binds much more tightly to the intracellular zinc metalloregulatory protein from *E. coli*, ZntR ($K_d^{Zn} \sim 10^{-15}$ M) (*58*). The coordination environment of this tight zinc-binding site has been characterized by Zn^{2+} extended X-ray absorption fine structure (EXAFS), and it features three sulfur ligands and an N/O ligand (*59*). The large difference in binding affinity exhibited by ZntR as compared to those of other zinc-binding sites suggests that protein environments can have a substantial impact on binding affinity and metal selectivity (*59*). In addition, the higher affinity observed in this system suggests that the concentration of bioavailable zinc in prokaryotes may be significantly lower than it is in the nuclei of eukaryotes.

CONCLUSIONS

Rigorous metal-binding studies conducted with hERα-DBD and GR-DBD indicate that Co^{2+} binds to both sites with roughly the same affinity (in each protein, $K_{d1}^{Co} \sim K_{d2}^{Co} \sim 10^{-7}$ M). Additionally, Zn^{2+} binds to each of the two sites

in the DNA-binding domains of steroid receptor proteins with approximately the same affinity (in each protein, $K_{d1}^{Zn} \sim K_{d2}^{Zn} \sim 10^{-10}$ M). These results suggest that there is relatively little interaction between the two metal sites with respect to metal binding, despite the fact that they are part of the same domain. The affinity of Co^{2+} and Zn^{2+} for these sites is slightly weaker than that to the consensus zinc-finger peptide CP-1 but is comparable to those for most other naturally occurring structural zinc-binding domains with CCHH (*24*, *27*) and CCHC sites (*27*, *29*).

ACKNOWLEDGMENT

Hilary Arnold Godwin is a Howard Hughes Professor and a recipient of a Camille and Henry Dreyfus New Faculty Award, a Burroughs Wellcome Fund New Investigator Award in the Toxicological Sciences, an NSF CAREER Award, a Sloan Research Fellowship, and a Camille Dreyfus Teacher-Scholar Award. The authors thank Dr. Barry Gehm (Northwestern University Medical School) and Prof. Pierre Chambon (Institut de Genetique et de Biologie Moleculaire et Cellulaire) for providing the cDNA for hERα and Dr. Richard Gaber (Department of Biochemistry, Molecular Biology, and Cell Biology at Northwestern University) for providing the cDNA for GR. DNA sequencing of the prokaryotic plasmid constructs was performed by Janelle Thorek in the Northwestern University Biotechnology Laboratory. The authors thank Prof. Tom O'Halloran and the members of his lab for allowing us to use their Cary 300 Bio UV−vis spectrophotometer. Absorption spectra were recorded at the Keck Biophysics Facility at Northwestern University [http://www.biochem.northwestern.edu/Keck/keckmain.html]. Inductively coupled plasma analyses were conducted with the assistance of Saman Shafaie, and mass spectrometry studies were conducted by Dr. Fenghe Qiu in the Analytical Services Laboratory (ASL) at Northwestern University. Finally, the authors thank Drs. John Magyar and Amy Ghering for insightful discussions.

SUPPORTING INFORMATION AVAILABLE

Absorption spectra collected for the direct Co^{2+} titrations of hERα-DBD and GR-DBD showing the presence of Cys $S^- \rightarrow Co^{2+}$ LMCT bands; a detailed view of the Co^{2+} d → d electronic transitions resulting from a Co^{2+} titration of GR-DBD; absorption spectra collected during a Co^{2+} competition experiment between GR-DBD and CP-1; Zn^{2+} titration of GR-DBD; circular dichroism spectra of apo, Zn, and Co forms of hERα-DBD and GR-DBD; and electrophoretic mobility shift assays of apo, Zn, and Co forms of hERα-DBD and GR-DBD with their corresponding hormone response element DNA. This material is available free of charge via the Internet at http://pubs.acs.org.

REFERENCES

1. Schwabe, J. W. R., and Rhodes, D. (1991) Beyond zinc fingers: steroid hormone receptors have a novel structural motif for DNA recognition, *Trends Biochem. Sci. 16*, 291−296.
2. Clarke, N. D., and Berg, J. M. (1998) Zinc fingers in *Caeborhabditis elegans*: finding families and probing pathways, *Science 282*, 2018−2022.
3. Laudet, V., Hanni, C., Coll, J., Catzeflis, F., and Stehelin, D. (1992) Evolution of the nuclear receptor gene superfamily, *EMBO J. 11*, 1003−1013.
4. Evans, R. M. (1988) The steroid and thyroid hormone receptor superfamily, *Science 240*, 889−895.
5. Katzenellenbogen, J. A., and Katzenellenbogen, B. S. (1996) Nuclear hormone receptors: ligand-activated regulators of transcription and diverse cell responses, *Chem. Biol. 3*, 529−536.
6. Mangelsdorf, D. J., Thummel, C., Beato, M., Herrlich, P., Schütz, G., Umesono, K., Blumberg, B., Kastner, P., Mark, M., Chambon, P., and Evans, R. M. (1995) The nuclear receptor superfamily: the second decade, *Cell 83*, 835−839.
7. Schwabe, J. W. R., Neuhaus, D., and Rhodes, D. (1990) Solution structure of the DNA-binding domain of the oestrogen receptor, *Nature 348*, 458−461.
8. Baumann, H., Paulsen, K., Kovács, H., Berglund, H., Wright, A. P. H., Gustafsson, J. Å., and Härd, T. (1993) Refined solution structure of the glucocorticoid receptor DNA-binding domain, *Biochemistry 32*, 13463−13471.
9. Schwabe, J. W. R., Chapman, L., Finch, J. T., and Rhodes, D. (1993) The crystal structure of the estrogen-receptor DNA-binding domain bound to DNA—how receptors discriminate between their response elements, *Cell 75*, 567−578.
10. Luisi, B. F., Xu, W. X., Otwinowski, Z., Freedman, L. P., Yamamoto, K. R., and Sigler, P. B. (1991) Crystallographic analysis of the interaction of the glucocorticoid receptor with DNA, *Nature 352*, 497−505.
11. Sabbah, M., Redeuilh, G., Secco, C., and Baulieu, E.-E. (1987) The binding activity of estrogen receptor to DNA and heat shock protein (M_r 90 000) is dependent on receptor-bound metal, *J. Biol. Chem. 262*, 8631−8635.
12. Berg, J. M., and Shi, Y. (1996) The galvanization of biology: a growing appreciation for the roles of zinc, *Science 271*, 1081−1085.
13. Freedman, L. P., Luisi, B. F., Korszun, Z. R., Basavappa, R., Sigler, P. B., and Yamamoto, K. R. (1988) The function and structure of the metal coordination sites within the glucocorticoid receptor DNA-binding domain, *Nature 334*, 543−546.
14. Low, L. Y., Hernández, H., Robinson, C. V., O'Brien, R., Grossmann, J. G., Ladbury, J. E., and Luisi, B. (2002) Metal-dependent folding and stability of nuclear hormone receptor DNA-binding domains, *J. Mol. Biol. 319*, 87−106.
15. Semenza, G. L. (1994) Transcriptional regulation of gene expression: mechanisms and pathophysiology, *Hum. Mutat. 3*, 180−199.
16. Lubahn, D. B., Moyer, J. S., Golding, T. S., Couse, J. F., Korach, K. S., and Smithies, O. (1993) Alteration of reproductive function but not prenatal sexual development after insertional disruption of the mouse estrogen receptor gene, *Proc. Natl. Acad. Sci. U.S.A. 90*, 11162−11166.
17. Beato, M., Herrlich, P., and Schütz, G. (1995) Steroid hormone receptors: many actors in search of a plot, *Cell 83*, 851−857.
18. Burris, T. P., and McCabe, E. R. B. (2001) Nuclear receptors and genetic diseases, Academic Press, San Diego.
19. Liang, X., Lu, B., Scott, G. K., Chang, C.-H., Baldwin, M. A., and Benz, C. C. (1998) Oxidant stress impaired DNA-binding of estrogen receptor from human breast cancer, *Mol. Cell. Endocrinol. 146*, 151−161.
20. Lippard, S. J., and Berg, J. M. (1994) *Principles of bioinorganic chemistry*, University Science Books, Sausalito, CA.
21. Vallee, B. L., and Holmquist, B. (1980) in *Methods for Determining Metal Ion Environments in Proteins: Structure and Function of Metalloproteins* (Darnall, D. W., and Wilkins, R. G., Eds.), Elsevier/North-Holland, New York.
22. Vašák, M., Kägi, J. H. R., Holmquist, B., and Vallee, B. L. (1981) Spectral studies of cobalt(II)- and nickel(II)-metallothionein, *Biochemistry 20*, 6659−6664.
23. Predki, P. F., and Sarkar, B. (1992) Effect of replacement of "zinc finger" zinc on estrogen receptor DNA interactions, *J. Biol. Chem. 267*, 5842−5846.
24. Berg, J. M., and Merkle, D. L. (1989) On the metal ion specificity of "zinc finger" proteins, *J. Am. Chem. Soc. 111*, 3759−3761.
25. Frankel, A. D., Berg, J. M., and Pabo, C. O. (1987) Metal-dependent folding of a single zinc finger from transcription factor IIIA, *Proc. Natl. Acad. Sci. U.S.A. 84*, 4841−4845.
26. Krizek, B. A., Amann, B. T., Kilfoil, V. J., Merkle, D. L., and Berg, J. M. (1991) A consensus zinc finger peptide—design, high-affinity metal-binding, a pH-dependent structure, and a His to Cys sequence variant, *J. Am. Chem. Soc. 113*, 4518−4523.
27. Krizek, B. A., Merkle, D. L., and Berg, J. M. (1993) Ligand variation and metal-ion binding specificity in zinc finger peptides, *Inorg. Chem. 32*, 937−940.
28. Michael, S. F., Kilfoil, V. J., Schmidt, M. H., Amann, B. T., and Berg, J. M. (1992) Metal binding and folding properties of a minimalist Cys_2His_2 zinc finger peptide, *Proc. Natl. Acad. Sci. U.S.A. 89*, 4796−4800.

29. Green, L. M., and Berg, J. M. (1989) A retroviral Cys-Xaa_2-Cys-Xaa_4-His-Xaa_4-Cys peptide binds metal ions: spectroscopic studies and a proposed three-dimensional structure, *Proc. Natl. Acad. Sci. U.S.A. 86*, 4047−4051.
30. Green, L. M., and Berg, J. M. (1990) Retroviral nucleocapsid protein−metal ion interactions: folding and sequence variants, *Proc. Natl. Acad. Sci. U.S.A. 87*, 6403−6407.
31. Chen, X., Chu, M., and Giedroc, D. P. (2000) Spectroscopic characterization of Co(II)-, Ni(II)-, and Cd(II)-substituted wild-type and non-native retroviral-type zinc finger peptides, *J. Biol. Inorg. Chem. 5*, 93−101.
32. Roehm, P. C., and Berg, J. M. (1997) Sequential metal binding by the RING finger domain of BRCA1, *Biochemistry 36*, 10240−10245.
33. Lai, Z. H., Freedman, D. A., Levine, A. J., and McLendon, G. L. (1998) Metal and RNA binding properties of the hdm2 RING finger domain, *Biochemistry 37*, 17005−17015.
34. Berkovits, H. J., and Berg, J. M. (1999) Metal and DNA binding properties of a two-domain fragment of neural zinc finger factor 1, a CCHC-type zinc-binding protein, *Biochemistry 38*, 16826−16830.
35. Blasie, C. A., and Berg, J. M. (2000) Toward ligand identification within a CCHHC zinc-binding domain from the NZF/MyT1 family, *Inorg. Chem. 39*, 348−351.
36. Kumar, V., Green, S., Stack, G., Berry, M., Jin, J. R., and Chambon, P. (1987) Functional domains of the human estrogen receptor, *Cell 51*, 941−951.
37. The amino acid sequence of the hERα-DBD polypeptide (residues 121−280 of hERα) is LQPHGQQVPYYLENEPSGYTVREAG-PPAFYRPNSDNRRQGGRERLASTNDKGSMAMESAKETRYC-AVCNDYASGYHYGVWSCEGCKAFFKRSIQGHNDYMCPA-TNQCTIDKNRRKSCQACRLRKCYEVGMMKGGIRKDRRGG-RMLKHKRQRDDGEGRGEV.
38. Oligonucleotide primer prepared by Integrated DNA Technologies, Inc. Coralville, IA. Sequence: 5′-AAT AG**G GAT CC**C TGC AGC CCC ACG GCC AGC AG-3′. A *Bam*HI restriction site is shown in boldface.
39. Oligonucleotide primer prepared by Integrated DNA Technologies, Inc. Coralville, IA. Sequence: 5′-TGT TC**G AAT TC**T CAC ACT TCA CCC CTG CCC TCC CC-3′. An *Eco*RI restriction site is shown in boldface.
40. Sehgal, B. U., Dunn, R., Hicke, L., and Godwin, H. A. (2000) High-yield expression and purification of recombinant proteins in bacteria: a versatile vector for glutathione-*S*-transferase fusion proteins containing two protease cleavage sites, *Anal. Biochem. 281*, 232−234.
41. Nathan, D. F., and Lindquist, S. (1995) Mutational analysis of Hsp90 function−interactions with a steroid receptor and a protein kinase, *Mol. Cell. Biol. 15*, 3917−3925.
42. The amino acid sequence of the GR-DBD polypeptide (residues 425−515 of GR) is GSPPSSSSAATGPPPKLCLV-CSDEASGCHYGVLTCGSCKVFFKRAVEGQHNYLCAGRN-DCIIDKIRRKNCPACRYRKCLQAGMNLEARKTKK.
43. Oligonucleotide primer prepared by Integrated DNA Technologies, Inc. Coralville, IA. Sequence: 5′-AAT AG**G GAT CC**C CTC CAT CCA GCT CGT CAG CA-3′. A *Bam*HI restriction site is shown in boldface.
44. Oligonucleotide primer prepared by Integrated DNA Technologies, Inc. Coralville, IA. Sequence: 5′-TTA CC**G AAT TC**T CAT TTC TTT GTT TTT CGA GCT TC-3′. An *Eco*RI restriction site is shown in boldface.
45. The sequence for the zinc finger consensus peptide (CP-1) is PYKCPECGKSFSQKSDLVKHQRTHTG.
46. Riddles, P. W., Blakeley, R. L., and Zerner, B. (1983) Reassessment of Ellman's reagent, *Methods Enzymol. 91*, 49−60.
47. The molar extinction coefficient for the Co−CP−CCHH complex was provided by J. M. Berg and co-workers (personal communication).
48. Magyar, J. S., and Godwin, H. A. (2003) Analysis of metal binding to structural zinc-binding sites: accounting quantitatively for pH and metal ion buffering effects, *Anal. Biochem. 320*, 39−54.
49. SPECFIT/32 is a product of Spectrum Software Associates and is owned solely by the authors, Robert Binstead, Andreas Zuberbuhler, and Bernhard Jung.
50. Scheller, K. H., Abel, T. H. J., Polanyi, P. E., Wenk, P. K., Fischer, B. E., and Sigel, H. (1980) Metal ion/buffer interactions. Stability of binary and ternary complexes containing 2-[Bis(2-hydroxyethyl)amino]-2(hydroxymethyl)-1,3-propanediol (BisTris) and Adenosine 5′-Triphosphate (ATP), *Eur. J. Biochem. 107*, 455−466.
51. Guo, J., and Giedroc, D. P. (1997) Zinc site redesign in T4 gene 32 protein: structure and stability of cobalt(II) complexes formed by wild-type and metal ligand substitution mutants, *Biochemistry 36*, 730−742.
52. Klotz, I. M. (1997) *Ligand receptor energetics: a guide for the perplexed*, John Wiley, New York.
53. Davis, W. J., and Smith, J. (1971) Imidazole complexes with cobalt(II) salts, *J. Chem. Soc. A.* 317−324.
54. Lane, R. W., Ibers, J. A., Frankel, R. B., Papaefthymiou, G. C., and Holm, R. H. (1977) Synthetic analogues of the active sites of iron−sulfur proteins. 14. [1]Synthesis, properties, and structures of bis(*o*-xylyl-α,α′-dithiolato)ferrate(II,III) anions, analogues of oxidized and reduced rubredoxin sites, *J. Am. Chem. Soc. 99*, 84−98.
55. Payne, J. C., ter Horst, M. A., and Godwin, H. A. (1999) Lead fingers: Pb^{2+} binding to structural zinc-binding domains determined directly by monitoring lead-thiolate charge-transfer bands, *J. Am. Chem. Soc. 121*, 6850−6855.
56. McLendon, G., Hull, H., Larkin, K., and Chang, W. (1999) Metal binding to the HIV nucleocapsid peptide, *J. Biol. Inorg. Chem. 4*, 171−174.
57. Buchsbaum, J. C., and Berg, J. M. (2000) Kinetics of metal binding by a zinc finger peptide, *Inorg. Chim. Acta 297*, 217−219.
58. Hitomi, Y., Outten, C. E., and O'Halloran, T. V. (2001) Extreme zinc-binding thermodynamics of the metal sensor/regulator protein, ZntR, *J. Am. Chem. Soc. 123*, 8614−8615.
59. Outten, C. E., Tobin, D. A., Penner-Hahn, J. E., and O'Halloran, T. V. (2001) Characterization of the metal receptor sites in *Escherichia coli* Zur, an ultrasensitive zinc(II) metalloregulatory protein, *Biochemistry 40*, 10417−10423.

BI035002L